Thermal Conductivity of Comets

G. N. Kumar*
Auburn University, Auburn, Ala.

and

M. S. Khader†
Cairo University, Cairo, Egypt

and

R. I. Vachon‡
Aurburn University, Auburn, Ala.

The thermal conductivity of two comet models is calculated. Both models assume the comets to be heterogeneous in composition. One model considers the comet to have a nucleus of water-ice mixed with meteoroid materials in the form of dust and agglomerated particles surrounded by a layer of water-frost. The second model assumes the frost and water-ice layers have sublimated, leaving a porous structure to some depth composed of solid meteoroid materials with residual gases. K values are calculated as a function of depth, density, temperature, and porosity.

Nomenclature

B = constant in Eqs. (2) and (4)
C = constant in Eqs. (2) and (4)
C' = negative of C
K = thermal conductivity (w/cm-K)
P = phase volume fraction
P_l = porosity
P_m = mass fraction = mass of meteoroid materials/mass of (meteoroid materials + water-ice)
R = thermal resistance
T = absolute temperature (K)
E = modulus of elasticity of solid particle
g = gravitational constant
z = depth below the surface
ρ = density
$\bar{\rho}$ = average density
ν = Poisson's ratio

Subscripts

c = continuous phase
d = discontinuous phase
eff = effective

Introduction

A COMET is generally regarded to be composed of three primary regions: the nucleus or kernel, the coma (a plasma region surrounding the nucleus), and the tail. Since not much is known about the composition and structure of the nucleus, it is thought that some useful information may be inferred by investigating the heat and mass transfer of the nucleus. It is impossible to undertake such studies without knowledge of the material thermal properties of possible nucleus models. Two possible models are described.

Model I consists of a nucleus and a surrounding shell. The nucleus consists of a water-ice mixed with meteoroid materials in the form of dust and agglomerated particlates. The shell is a layer of water-frost.

Model II is similar to Model I except that it is assumed the frost layer and water-ice have been subliminating and evaporating, leaving a porous structure composed of the solid meteoroid materials with residual gases partially confined in the porous structure to varying amounts to some depth.

The objectives of the analyses performed herein are to recommend values for the thermal conductivity of: 1) the water-ice and meteoroid materials of Model I; and 2) the porous structure of Model II as a function of depth. The comets were: a) Encke with a minimum temperature of 140 K and radius of 4km; and b) Halley with a minimum temperature of 49 K and radius of 15km.

Analyses

Model I

The Cheng and Vachon Model[1] has been used to calculate the approximate effective thermal conductivity of the water-ice solid debris mixture layer for Model I. The nucleus of a comet is believed to consist of 70% or more of ices by mass and the rest, meteoroid materials.[2] In the absence of detailed information on the composition of the meteoroid material (other than that it might contain Fe, Ca, Mn, Mg, Cr, Si, Ni, Al, etc), the meteoroid materials have been approximated first with the properties of basalt and then with properties of basalt and iron which are mixed in different proportions. These two approximations are designated A and B.

Model I is simplified to a mixture of water-ice and basaltic material when the solid debris has been approximated with the properties of basalt. This simplified model is designated Model I (A). Since the temperature of the nucleus varies with its distance from the sun (ex.—at alphelion[3] temperature of nucleus of Encke = 142 K and that of Halley = 49 K), the thermal conductivities have been calculated for the various

Presented as Paper 75-199 at the AIAA 13th Aerospace Sciences Meeting, Washington, D. C., January 20-22, 1975; submitted January 24, 1975; revision received April 17, 1975. The authors wish to acknowledge the support of B. Jones of the Space Sciences Laboratory, NASA Marshall Space flight Center, and the support of NASA under Contract NAS8-26579.

Index categories: Heat Conduction; Thermal Modeling and Experimental Thermal Simulation; Thermal Surface Properties.

*Graduate Assistant.
†Lecturer.
‡Professor.

assumed temperatures of the nucleus. The calculations have also been performed with varying proportions of ice and basaltic material.

Model I is simplified to a mixture of ice, basaltic material and iron when the solid debris is approximated by a mixture of basaltic material and iron. This simplified model is designated Model IB. Again the calculations have been performed for different assumed temperatures of the nucleus (variation of thermal properties within the nucleus for a given average temperature have not been considered) and for varying proportions of water-ice and solid debris. The calculations have also been performed with varying proportions of basalt and iron for a given ice, solid debris ratio.

A linear variation of thermal conductivity with temperature has been assumed for the water-ice and using the values given in Ref. 4. The following equations were obtained for the thermal conductivity and the density variation of ice with temperature:

$$K_{\text{ice}} = [0.0481156 - 9.244 \times 10^{-5} T]\ \text{w/cm} - \text{K} \qquad (1a)$$

$$\rho_{\text{ice}} = [0.94323 - 9.244 \times 10^{-5} T]\ \text{gm/cm}^3 \quad T \text{ in K} \qquad (1b)$$

The following property values were used for the basalt[5] and iron.[6] Basalt: $\rho = 2830$ kg/m^3; $E = 2.2 \times 10^{11}$ N/m^2; $K_s = 1.34$ w/m K; and $\nu = 0.2$.

Iron: $\rho = 7890$ kg/m^3; $E = 2.07 \times 10^{11}$ N/M^2; $K_s = 63.7$ w/m K; and $\nu = 0.3$. K_{ice} is of the order 3.8 w/m K at 100 K.

Model IA

The ratio $(K_{\text{ice}}/K_{\text{solid}})$ is in the range 1 to 4 for the temperature range of 30-200 K. Hence, from Ref. 1, for the case $K_c > K_d$ the effective or equivalent thermal resistance is given by

$$R_{\text{eff}} = \frac{2}{(-C'(K_d - K_c)\ [K_c + B(K_d - K_c)])^{1/2}} \times \tan^{-1} \frac{B}{2} \left[\frac{-C'(K_d - K_c)}{K_c + B(K_d - K_c)} \right]^{1/2} + \frac{1 - B}{K_c} \qquad (2)$$

where: K_c = thermal conductivity of continuous phase (water-ice in this case); K_d = thermal conductivity of discontinuous phase (basalt in this case); P_d = discontinuous phase volume fraction; $B = (3P_{d/2})^{1/2}$; $C = -4/B$; and $C' = -C$ and the approximate effective thermal conductivity is given by

$$K_{\text{eff}} = 1/R_{\text{eff}} \qquad (3)$$

K_{eff} has been calculated for different temperatures of nucleus and for different fractions of the discontinuous phase (basalt in this model).

Model IB

In Model IB, one has a three-phase mixture of water-ice, basalt and iron and it is necessary to find the approximate thermal conductivity (K_{eff}) of this three-phase mixture. Cheng and Vachon[1] give the following method for calculating K_{eff}:

The three-phase mixture is reduced to a two-phase mixture by considering that two of the phases can be combined and can be considered to be one phase of a two-phase system. The effective thermal conductivity of the two combined phases is determined and then the effective thermal conductivity of the two combined phases and the remaining phase is determined. This technique is seen in the following development.

Since the major portion of the comet nucleus is made up of water-ice, we take water-ice to be the continuous phase in applying the equation developed by Cheng and Vachon for 3 phase mixtures. Let: K_c = thermal conductivity of the continuous phase (i.e., of water-ice); K_{d_1} = thermal conductivity of the first discontinuous phase (i.e., of Fe); and K_{d_2} = thermal conductivity of the second discontinuous phase (i.e., of basalt). Thus, from the given range of values for the above, we have $(K_{d_1}/K_c) > 10$ and $(K_{d_2}/K_c) < 1$.

To determine the effective thermal conductivity (K_{eff}) of this 3-phase mixture, the 3-phase mixture is considered to be reduced to a 2-phase mixture in which the continuous phase is composed of the original continuous phase of the three-phase mixture and the second discontinuous phase. The discontinuous phase of this 2-phase mixture is the first discontinuous phase of the 3-phase mixture.

For this 2-phase mixture, $P_d = P_{d_1}$, $P_{ce} = P_c + P_{d_2}$, $K_d = K_{d_1}$, K_{ce} = thermal conductivity of the effective continuous phase, and P_{ce} = phase volume fraction of the effective continuous phase. K_{ce}, the effective thermal conductivity of the original continuous phase mixed with the second discontinuous phase of the 3-phase mixture, is determined as per the method outlined for Model IA.

Now, since $(K_{d_1}/K_{ce}) > 10$, from Ref. 1, the effective resistance R_{eff} is given by

$$R_{\text{eff}} = \frac{1}{\{C'(K_{d_1} - K_{ce})\ [K_{ce} + B_1 (K_{d_1} - K_{ce})]\}}$$

In

$$\frac{[K_{ce} + B_1(K_{d_1} - K_{ce})\}^{1/2}}{\{K_{ce} + B_1(K_{d_1} - K_{ce})\}^{1/2}} \frac{+ (B_1/2)\{C'(K_{d_1} - K_{ce})\}^{1/2}}{-(B_1/2)\{C'(K_{d_1} - K_{ce})\}^{1/2} + (1 - B_1/K_{ce})} \qquad (4)$$

where

$$B_1 = (3P_{d_1}/2)^{1/2}$$

and

$$C' = -C = +4/B_1$$

and the effective thermal conductivity is again given by

$$K_{\text{eff}} = 1/R_{\text{eff}} \qquad (3)$$

This calculation has been performed for different assumed temperature of the nucleus (here also, the thermal property variation inside the nucleus has not been considered) and for different phase volume fractions of the continuous phase. For a given value of phase volume fraction of water ice, calculations have been performed for varying proportions of basalt and iron.

Model II

It is now assumed for Model I that the frost layer and the water-ice has been sublimating and evaporating, which occurs as the comet nears the sun (distance less than 2 a.u.), thus leaving a porous structure.

A simplified approximation for the effective thermal conductivity, as a function of depth, is obtained using the theoretical model developed by Khader and Vachon[5] for heterogeneous mixtures. In the application of Ref. 5 to Model II case, it has been assumed that since the gas is at low pressure the thermal conductivity of the residual gases is quite small compared to the thermal conductivity of basalt and meteoritic material. Hence, the thermal conductivity through the void can be neglected. Also, since the temperatures involved are of the order of 100 K, radiation through the void space (i.e., through the gases at very low pressures) could be neglected as being very small in comparison to conduction through the solid.

Model IIA

Thus, with the simplifications just described and from Ref. 5, one obtains the following expression for the effective thermal conductivity when the solid is approximated with the properties of basalt.

$$K_{\text{eff}} = \frac{3(1-P_{l_s})(1-C_l^2 Z^{2/3})K_s}{[(\pi/2)((3/2C_l Z^{1/3})-1)+(4-1.2C_l^2 Z^{2/3})]} \quad (5)$$

where

$$C_l = [2\, g\bar{\rho}\pi(1-\nu^2)/16\, E(1-P)]^{1/3}$$

and $\bar{\rho}$ is average density of the solid; and P_{l_s} is porosity of the solid material. The calculations have been performed for different porosities and for different densities up to a depth of 2500 m.

Model IIB

When the solid material is approximated by a heterogeneous mixture of basalt and iron, the problem is solved in two stages. First, an effective value of thermal conductivity is obtained for the heterogeneous mixture of basalt and iron using the Cheng and Vachon model.[1]

Then the model for the second state consists of the solid material whose thermal conductivity was determined in Stage 1 and whose voids are assumed to be filled with low pressure residual gases. The effective thermal conductivity of this stage is determined using the Khader and Vachon model as explained for Model IIA.

Results and Discussion

Model IA

Figure 1 shows the variation of effective thermal conductivity with the average temperature when the solid debris is approximated with the properties of basalt for different values of the density of the discontinuous phase at a given value of mass fraction of the discontinuous phase (for example: Fig. 1 is for the case when there is 80% of water-ice and 20% of basalt by mass). This figure shows that the effective thermal conductivity of this layer is of the same order as that of water-ice and that its variation with temperature is also linear. The reason for this is that the major portion of the nucleus (about 70-80%) is made up of water-ice and the thermal conductivity of basalt is also of the same order of magnitude as that of water-ice. The figure also shows that at a given temperature there is not much variation in K_{eff} with change in density for this case, especially near temperature of the order of 200 K.

Figure 2 shows the variation of K_{eff} with mass fraction of solid debris (i.e., discontinuous phase approximated by basalt in this case). The figure shows that the variation is not appreciable in the range of mass fraction predicted for the nucleus of a comet and that there is a slight decrease in the thermal conductivity as mass fraction of solid debris is increased. This is because, for this model, the thermal conductivity of solid debris (approximated by basalt) is less than that of water-ice. Hence, as the mass fraction of solid debris increases, the effective thermal conductivity decreases. Figure 2 also shows that the variation is more pronounced at temperatures near 40 K than near 200 K where it is almost flat.

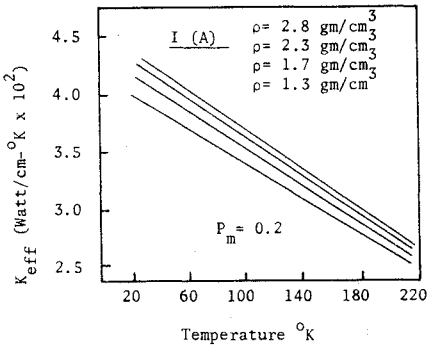

Fig. 1 Effective thermal conductivity at constant density.

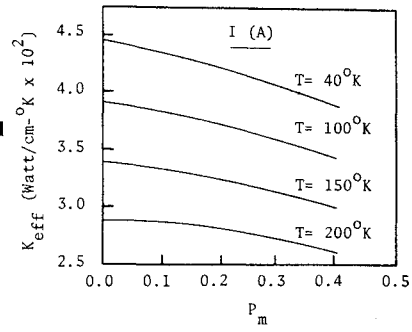

Fig. 2 Effective thermal conductivity variation with mass fraction.

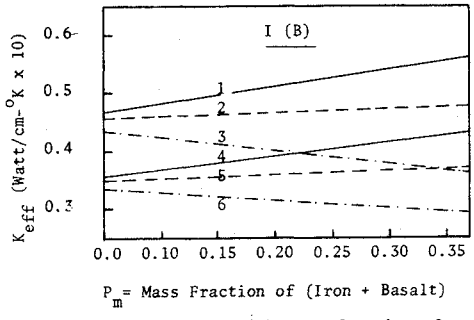

Fig. 3 Effective thermal conductivity as a function of mass fraction of solid debris: 1—water-ice + iron at $T = 50$ K; 2—water-ice + (iron and basalt) in ratio 1:1 at $T = 50$ K; 3— water-ice + basalt at $T = 50$ K; lines 4-6 at $T = 150$ K.

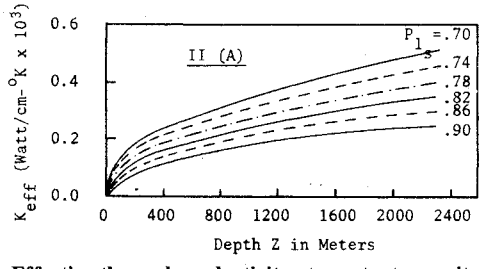

Fig. 4 Effective thermal conductivity at constant porosity with only basalt as solid material.

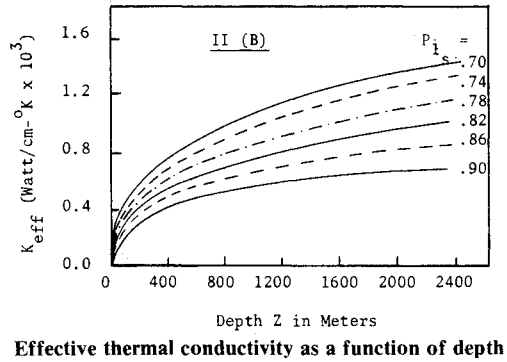

Fig. 5 Effective thermal conductivity as a function of depth at constant porosity with (iron and basalt) as solid materials in the ratio 1:1.

Model IB

For the model of IB, variation of thermal conductivity with the total mass fraction of basalt and iron is shown in Fig. 3 for different proportions of iron and basalt. As can be seen from this figure, although the curves start at almost the same

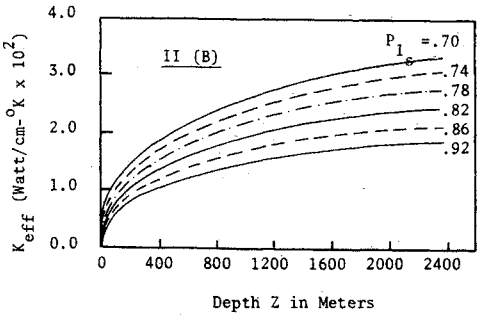

Fig. 6 Effective thermal conductivity as a function of depth at constant porosity with only iron as solid material.

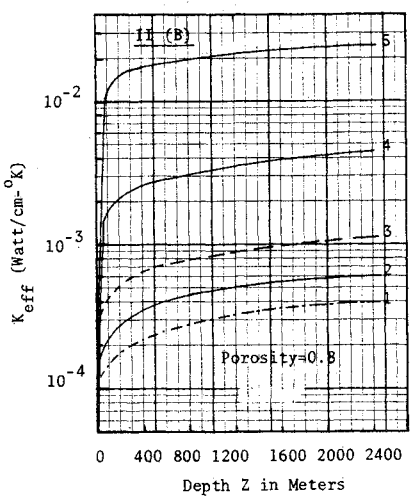

Fig. 7 Comparison of effective thermal conductivity for different proportions of basalt and iron as a function of depth at constant porosity: 1—with only basalt as the solid material; 2—with iron and basalt in the ratio 1:4; 3—with iron and basalt in the ratio 1:1; 4—with iron and basalt in the ratio 4:1; 5—with iron only as the solid material.

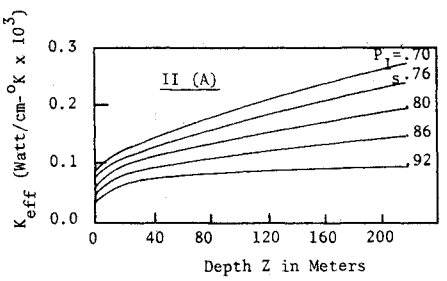

Fig. 8 Effective thermal conductivity as a function of depth at constant porosity with only basalt as solid material.

value of K_{eff} for very low values of mass fraction (the reason for which is that practically the whole nucleus in this case will be made up of water-ice), the slope of the curve changes from being negative for the model with only basalt, to positive for the model with only iron as the solid debris material. The reason for the positive slope in the latter case is that since the thermal conductivity of iron is much greater than that of water-ice, the thermal conductivity of the mixture increases as the percentage of iron increases. When iron and basalt are in the ratio 1:1, even though the slope is positive, the increase is not marked.

Model II

Figures 4-6 show the plots of variation of the effective thermal conductivity with depth for different values of porosity; each figure represents a particular proportion of iron and

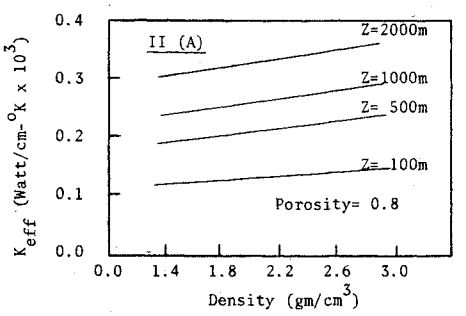

Fig. 9 Effective thermal conductivity as a function of density at constant depth with basalt as solid material.

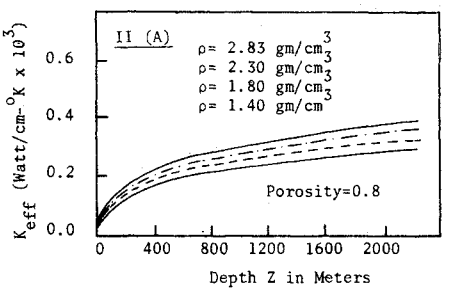

Fig. 10 Effective thermal conductivity as a function of depth at constant density with basalt as the solid material.

basalt. For this model, the mass fraction as previously defined (see Nomenclature) is 1.0. They all exhibit the same general trend of increase of K_{eff} with depth, the increase being sharper during the earlier part and then becoming gradual. The reason for this is that as the depth increases, the contact area between the particles increase due to the increase in loading and consequently smaller thermal contact resistance and in turn thermal conductivity increases. As the porosity increases, the amount of solid material per unit volume decreases, and hence thermal conductivity decreases with porosity.

A comparative study of Figs. 4-6 is made in Fig. 7. Comparing curves 1 and 5, we see that the thermal conductivity increases by a factor of about 75 when basalt is replaced by iron. This marked increase in K_{eff} with increase in percentage of iron compared to basalt is because of the very high value of thermal conductivity for iron compared to basalt. This figure also shows that the curve of K_{eff} sharply rises for the first few hundred m and then becomes very gradual (almost flat). Thus after about 500 m, the effect of depth on thermal conductivity is not pronounced. This is because after this depth, no appreciable increase in contact area between the particles occurs with depth.

Figure 8 shows the variation of effective thermal conductivity with depth for the case IIA (i.e., with only basalt as solid material) for the first 200 m from the surface. This shows that even though the graph still follows the trend of Figs. 4, 5, and 6, actually the major portion of the increase in the value of K_{eff} takes place within a few meters from the surface and afterwards the increase is very gradual. Since the same pattern was followed for other cases (for varying proportions of basalt and iron), they have not been plotted.

Figure 9 illustrates the variation of K_{eff} with density at different depths when the solid material was approximated with the properties of basalt. The increase in thermal conductivity with density is very gradual and the reason for the increase in K_{eff} with density is the increased contact area between the particles, which in turn is due to increase in loading due to heavier mass/unit volume at a given porosity.

Figure 10 illustrates the variation of K_{eff} with depth for different densities for Model IIA. This figure shows that the increase in K_{eff} with depth is significant only at smaller depths

and becomes very gradual as the depth is increased. The reason for the increase in K_{eff} with depth is the same as that given Figs. 4-6. The increase with depth becomes gradual at greater depths because the increase in contact area with depth becomes very small at greater depths.

Conclusion

The results presented herein are indicative of the trends of the thermal conductivity data for comets. The results are predicted on postulated models for two comets. The data and analysis technique may prove helpful in the analysis of comets and ultimately may help establish accurate models for comets. Thus, hopefully the work reported can be of value to the iterative process of understanding the composition of comets through observations coupled with analyses.

References

[1]Cheng, S. C. and Vachon, R. I., "The Prediction of the Thermal Conductivity of Two and Three Phase Solid Heterogeneous Mixtures," *International Journal of Heat Mass Transfer*, Vol. 12, March 1969, pp. 249-264.

[2]Whipple, F. L., "A Comet Model II—Physical Relations for Comets and Meteors," *Astrophysical Journal*, Vol. 113, May 1951, pp. 464-474.

[3]Minnaret, M. G. J., "On the Temperature of the Cometary Nucleii," *Proceedings of the Academy of Sciences, Amsterdam*, No. 50, p. 826, 1947.

[4]Lentz, C. P., "Thermal Conductivity of Meats, Fats, Gelatin, Gels and Ice," *Food Technology*, Vol. 15, 1961, pp. 243-244.

[5]Khader, M. S. and Vachon, R. I., "A Theoretical Model for Lunar Surface Material Thermal Conductivity," Paper 73-HT-35, ASME Heat Transfer Conference, Atlanta, Ga., Aug. 1973.

[6]Eckert, E. R. G. and Drake, R. M., *Analysis of Heat and Mass Transfer*, McGraw-Hill, New York, 1972.